

## Supplement: The impact of relevant parameters in the controller on the results

We provide theoretical analysis and simulation results to analyze the impact of parameters  $\lambda$ ,  $\eta$ ,  $\xi_0$ , and  $\xi_1$  in the controller on the control.

### • Theoretical analysis

In the paper, for  $\lambda$ , it can be inferred from Eq.(10) and Eq.(15) ( $S = \tan(\frac{\pi}{2} \frac{z}{\rho(t)})$  (10),  $V = \frac{1}{2} S^2$  (15)) that if  $V$  is bounded, then  $S$  is bounded, i.e.,  $-\rho(t) < z < \rho(t)$ . According to the definition of  $z$  (i.e.,  $z = \lambda x_1 + x_2 - \lambda y_d$ ), it is known that  $x_1$  tracks  $y_d$  with an error of  $(-\rho(t) - x_2)/\lambda < x_1 - y_d < (\rho(t) - x_2)/\lambda$ , and the larger the value of  $\lambda$ , the smaller the error. For  $\eta$ , from the stability analysis on pages 5 to 6, one can be concluded that

$$\dot{V} \leq \frac{|S|\pi}{2\rho^2 \cos^2\left(\frac{\pi}{2} \frac{z(t)}{\rho}\right)} \left( \bar{\Gamma} - \rho(t)g\eta\ell'(t)o_4(t)|S| \right) \quad (1)$$

$$= \frac{\rho(t)g\eta\ell'(t)o_4(t)|S|\pi}{2\rho^2 \cos^2\left(\frac{\pi}{2} \frac{z(t)}{\rho}\right)} \left( \frac{\bar{\Gamma}}{\rho(t)g\eta\ell'(t)o_4(t)} - |S| \right). \quad (2)$$

From (2), it can be seen that the larger  $\eta$  is, the smaller  $\frac{\bar{\Gamma}}{\rho(t)g\eta\ell'(t)o_4(t)}$  is, thus the smaller  $|S|$  is more conducive to the stability of the system. However, from the design of the control law  $v(t) = -\eta S$ , it can be inferred that the larger  $\eta$  and  $|v|$ , the more severe the control chattering.  $\xi_0$  and  $\xi_1$  are the initial values and prescribed boundaries of the designed prescribed performance function  $\rho(t)$ , respectively. From  $v = -\eta S$  and  $S = \tan(\frac{\pi}{2} \frac{z}{\rho(t)})$ , it can be seen that the smaller  $\xi_0$ , the closer  $z(0)$  is to  $\rho(0)$ , and the larger  $v(0)$ , which means that the initial position chattering of the control is more severe. In addition, the smaller the corresponding  $\xi_0$ , the smaller the prescribed boundary range in  $t \in [0, t_\xi]$ , and the smaller the initial error. From  $(-\rho(t) - x_2)/\lambda < x_1 - y_d < (\rho(t) - x_2)/\lambda$ , it can be seen that when  $\lambda$  remains constant, the smaller  $\xi_1$ , the smaller the error in  $t > t_\xi$ .

### • Simulation result

In order to provide a more intuitive explanation of the results brought about by the changes in the above parameters, we have provided some comparative simulation results.

#### Simulation parameters selection

##### 1) The SbW system parameters selection

The specific simulation model of SbW systems can be found in [1]. The parameters of (1) are chosen as  $\mathcal{J}_f = 3.8\text{kg} \cdot \text{m}^2$ ,  $\mathcal{J}_m = 0.0045\text{kg} \cdot \text{m}^2$ ,  $\mu = 18$  and  $\mathcal{B}_m = 0.018 \cdot \text{s/rad}$ .  $\mathcal{H}_f(\theta_f, \dot{\theta}_f) = \tau_e + \tau_f$ , in which the friction torque  $\tau_f$  is considered as [1], i.e.,  $\tau_f = 0.25(\tanh(100x_2) - \tanh(x_2)) + 30\tanh(100x_2) + 10x_2$ , the self-aligning torque  $\tau_e$  is considered as Appendix B, the drive torque  $T_{fi} = 50\text{N} \cdot \text{m}$ ,  $i = r, l$ , the initial vehicle speed and wheel rotation speed are  $v_x = 19 \text{ m/s}$  and  $\omega = 57 \text{ rad/s}$ , respectively, the mechanical and pneumatic trail  $t_p = 0.023$ ,  $t_m = 0.016$ , and the other parameters are given in [2] and Tab.I. The input nonlinearity of (2) are chosen as  $\ell(t) = \ell_f \ell_r$  for  $u(t) \geq -\varsigma_l$ ;  $\ell(t) = \ell_f \ell_l$  for  $u(t) < -\varsigma_l$ ,  $\varsigma(t) = \varsigma_f(t) - \ell_f \ell_r \varsigma_r$  for  $u(t) > \varsigma_r$ ;  $\varsigma(t) = \varsigma_f(t) - \ell_f \ell_r u(t)$  for  $-\varsigma_l \leq u(t) \leq \varsigma_r$ ;  $\varsigma(t) = \varsigma_f(t) + \ell_f \ell_l \varsigma_l$  for  $u(t) < -\varsigma_l$ , where  $\ell_l = 1.2$ ,  $\ell_r = 1.4$ ,  $\varsigma_l = 40$  and  $\varsigma_r = 30$ , and  $\ell_f = 1$ ,  $\varsigma_f(t) = 0$  for  $t \in [0, 5]\text{s}$ ;  $\ell_f = 0.75$ ,  $\varsigma_f(t) = 3\sin(4t)$  for  $t \in [5, 10]\text{s}$ ;  $\ell_f = 0.5$ ,  $\varsigma_f(t) = 4\sin(3t)$  for  $t \in [10, 15]\text{s}$ ;  $\ell_f = 0.25$ ,  $\varsigma_f(t) = 3\sin(4t)$  for  $t \in [15, 20]\text{s}$ . Besides, the disturbance is assumed as  $d(t) = 5 \int [d_m - d(t) + 2\text{rand}(1)]dt$  with  $d_m = 2\cos(6t)$  for  $t \in [0, 5]$ ;  $d_m = 2.5\cos(4t)$  for  $t \in [5, 10]$ ;  $d_m = 3\cos(4t)$  for  $t \in [10, 15]$ ;  $d_m = 3.5\cos(4t)$  for  $t \in [15, 20]$ .

##### 2) Controller parameters selection

The prescribed performance control design (9)-(13) in simulation, the positive constants  $\lambda = 60$ ,  $\eta = 50$ ,  $\xi_0 = 10$ ,  $\xi_1 = 0.09$ , and the preseted steady-state time  $t_\xi = 0.2$ . Finally, the parameters of the event-triggering mechanism are designed as  $\varrho = 0.04$ ,  $m = 4$ , and  $\kappa = 10$ . Besides, the desired signal is selected as  $y_d = 0.3\sin(0.3t) \text{ rad}$ , with an initial value of  $x = [0.1, 0]^T$ .

##### 3) State quantizer and input quantizer parameters selection

TABLE I  
NOMENCLATURE

Notations	Descriptions	Value
$m$	Total mass of the vehicle	1298.9kg
$m_s$	Sprung mass of the vehicle	1167.5 kgm <sup>2</sup>
$I_{zz}$	Moment of inertia of the vehicle about the yaw axis	1627 kgm <sup>2</sup>
$I_{xx}$	Moment of inertia of the vehicle about the roll axis	498.9 kg m <sup>2</sup>
$I_{xz}$	Sprung mass product of the inertia	0 kgm <sup>2</sup>
$l_f$	Distance of the centre of gravity from the front axle	1 m
$l_r$	Distance of the centre of gravity from the rear axle	1.454 m
$d_f$	Front track width	1.436 m
$d_r$	Rear track width	1.436 m
$h$	Height of the centre of gravity of the sprung mass	0.533 m
$h_s$	Distance of the centre of gravity of the sprung mass from the roll axes	0.4572 m
$R_w$	Radius of the wheel	0.35 m
$I_w$	Moment of inertia of the wheel	2.1 kg · m <sup>2</sup>
$C_\alpha$	Cornering stiffness of one tyre	30,000 N/rad
$C_s$	Longitudinal stiffness of one tyre	50,000 N/unit slip
$k_{rsf}$	Front roll steer coefficient	-0.2 rad/rad
$k_{rsr}$	Rear roll steer coefficient	0.2 rad/rad
$K_R$	Ratio of the front roll stiffness to the total roll stiffness	0.552
$c_\varphi$	Torsional damping of the roll axis	3511.6 Nm/s
$k_\varphi$	Torsional stiffness of the roll axis	66,185.8 Nm/rad
$\varepsilon_r$	Road adhesion reduction factor	0.015 s/m
$g$	Acceleration due to gravity	9.81 m/s <sup>2</sup>
$\mu$	Nominal friction coefficient between the tyre and the ground	0.7
$T_i$	Driving torque of each wheel	50N · m
$v_x(0)$	Initial vehicle speed	19m/s
$w_i(0)$	Initial rotation speed of each wheel	57rad/s
$t_p$	Pneumatic trail	0.016
$t_m$	Mechanical trail	0.023

The parameters of state quantizer (4) are selected as  $\lambda = 60$  and  $\psi = 0.01$ . Besides, the parameters of the input quantizer (5) are selected as  $\beta = 0.8$  and  $v_{min} = 0.2$  in different simulations. The detailed simulation process and parameter calculation are shown in Tab. II.

#### 4) Different parameter selection

Only make changes to the following parameters while ensuring that all other parameters are the same:

$$\left\{ \begin{array}{l} \lambda = 30 \quad \text{and} \quad \lambda = 60 \\ \eta = 13, \quad \eta = 50, \quad \text{and} \quad \eta = 150. \\ \xi_0 = 10 \quad \text{and} \quad \xi_0 = 20. \\ \xi_1 = 0.09 \quad \text{and} \quad \xi_1 = 0.18. \end{array} \right. \quad (3)$$

Note: All "(·)" in this paper represent corresponding equations and can be found in the "Low-Complexity Quantized Prescribed Performance Control for Constrained Steer-by-Wire Systems with Input Nonlinearity and Bandwidth Limitations" paper.

#### Simulation results and analysis

TABLE II  
SIMULATION PROCESS AND PARAMETER CALCULATION

Step	Calculate
<b>State quantizer (4):</b> $x_1 \rightarrow Q_x(\chi)$	
Step 1	Input of state quantizer: $\chi = 60x_1 + \dot{x}_1$
Step 2	Case I: $Q_x(\chi) = L_i$ , Case II: $Q_x(\chi) = 0$ , Case III: $Q_x(\chi) = -L_i$
Designed parameters	$\lambda = 60$ , and $\psi = 0.01$ .
<b>Computational control law (9)-(11):</b> $Q_x(\chi) \rightarrow v(t)$	
Step 3	Error transformation: $z = Q_x(\chi) - 60y_d$
Step 4	Prescribed performance function: Case I: $\rho(t) = 0.08 + (7 - 0.08)\exp(-t/(0.1 - t))$ , Case II: $\rho(t) = 0.08$
Step 5	Control law: $v(t) = -100 \tan((\pi z(t))/(2\rho(t)))$
Designed parameters	$\lambda = 60$ , $\eta = 50$ , $\xi_0 = 10$ , $\xi_1 = 0.09$ , $t_\xi = 0.2$ , $y_d = 0.3\sin(0.3t)$ rad, and $x = [0.1, 0]^T$ .
<b>Input quantizer (5):</b> $v(t) \rightarrow Q_v(v)$	
Step 6	Case I: $Q_v(v) = v_i$ , Case II: $Q_v(v) = v_i(1 + \varpi)$ , Case III: $Q_v(v) = 0$ , Case IV: $Q_v(v) = -Q_v(-v)$
Designed parameters	$\beta = 0.8$ , and $v_{min} = 0.02$ .
<b>ETM (12)-(13):</b> $Q_v(v) \rightarrow u(t)$	
Step 7	Case I: $u(t) = Q_v(v(t_k))$ , Case II: $u(t) = Q_v(v(t_k))$
Designed parameters	$\varrho = 0.04$ , $m = 4$ , and $\kappa = 10$ .
<b>The SbW system (3):</b> $u(t) \rightarrow x_1$	
Step 8	$\mathcal{H}_f(x) = \tau_e + \tau_f$
Step 9	$\mathcal{J}_e = 3.8 + 18^2 \times 0.0045$
Step 10	$f(x) = -(18^2 \times 0.018x_2 + \mathcal{H}_f(x))/\mathcal{J}_e$
Step 11	$g(t) = 18/\mathcal{J}_e$
Step 12	$d(t) = 5 \int [d_m - d(t) + 2rand(1)]dt$
Step 13	$\ddot{x}_1 = \dot{x}_2 = f(x) + g(t)\ell(t)u(t) + d(t)$
$\tau_e, \tau_f, d_m, \ell(t), \varsigma(t)$	Please see <i>The SbW system parameters selection</i> .

Fig. 1 and Tab. III show the comparative simulation results. From Fig. 1(a) and Tab. III, it can be seen that as  $\lambda$  increases, it leads to smaller tracking errors (Note that  $y = x_1$  in the figure). Fig. 1(b) and Tab. III show the effect of different values of  $\eta$  on the control quantity  $u(t)$  and tracking error. It can be seen that the larger  $\eta$ , the more severe the chattering of the  $u(t)$ . In addition, Fig. 1(c) shows that a smaller value of  $\eta$  cannot guarantee the tracking performance of the system (note that theoretical analysis shows stability of the system for  $\eta > 0$ , but discrete points are used in simulation, so a smaller value of  $\eta$  may lead to system instability). Fig. 1(d) and Tab. III show that the larger the value of  $\xi_0$ , the larger the initial error boundary of the constraint, and after the prescribed time (i.e.,  $t_\xi = 0.2$ ), the error boundary and error variation of both are the same, and Tab. III shows that at  $t \in [0, 5]$ , the larger the value of  $\xi_0$ , the poorer the initial tracking performance. Fig. 1(e) shows that the initial chattering of the control with  $\xi_0 = 10$  is more severe. From Fig. 1(f) and Tab. III, it can be observed that the larger  $\xi_1$ , the larger the constraint boundary of the error, and the larger the error. It should be pointed out that the entire control result is affected by multiple parameters.

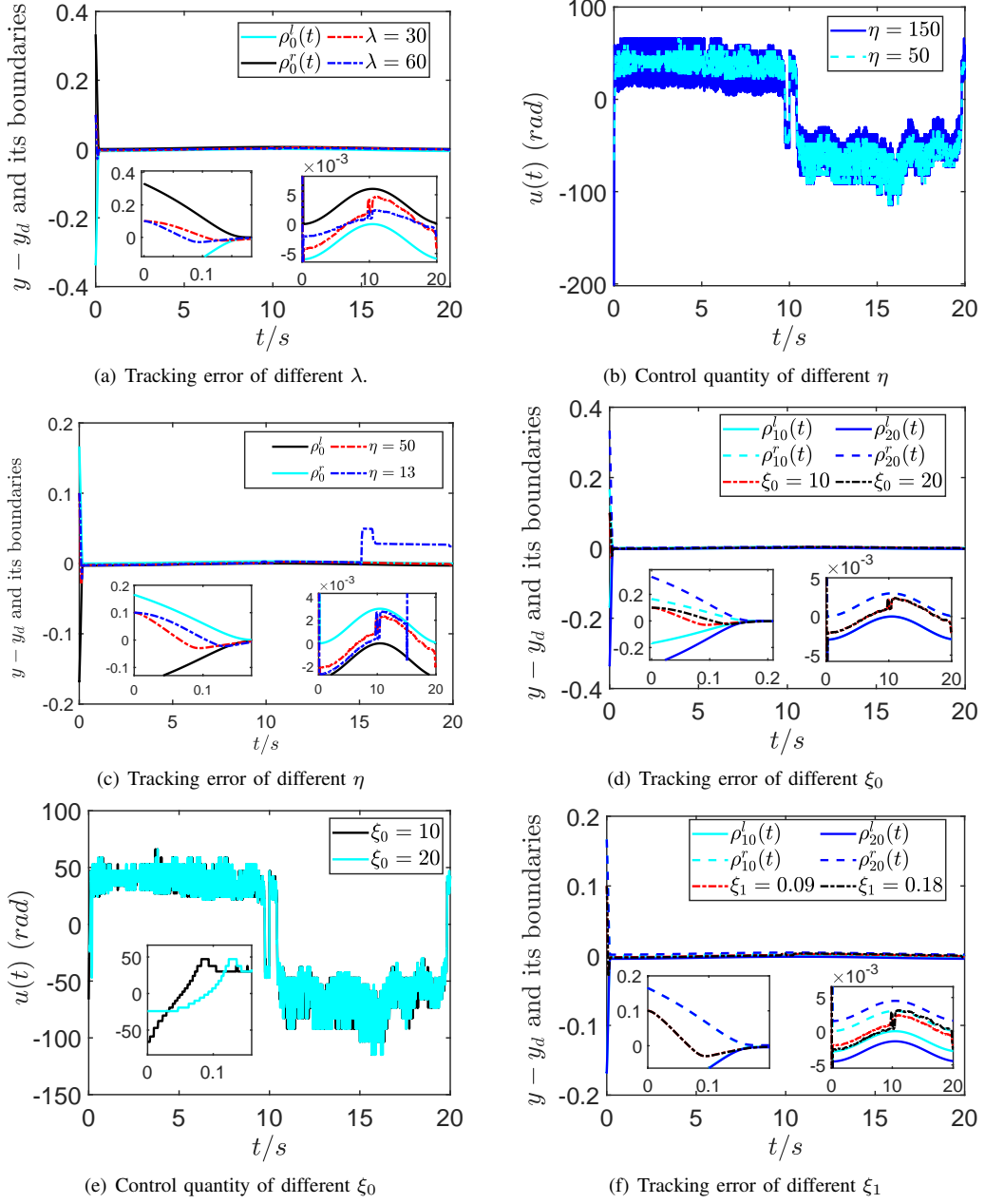


Fig. 1. Modeling of self-aligning torque.

## REFERENCES

- [1] B. Ma and Y. Wang, "Adaptive output feedback control of steer-by-wire systems with event-triggered communication," *IEEE/ASME Transactions on Mechatronics*, vol. 26, no. 4, pp. 1968–1979, 2021.
- [2] H. Du, J. Lam, K.-C. Cheung, W. Li, and N. Zhang, "Side-slip angle estimation and stability control for a vehicle with a non-linear tyre model and a varying speed," *Proceedings of The Institution of Mechanical Engineers Part D-journal of Automobile Engineering*, vol. 229, no. 4, pp. 486–505, 2015.

TABLE III  
ERROR INDICATORS OF IAE

	Different values of variables	$[0, 5)_s$	$[5, 10)_s$	$[10, 15)_s$	$[15, 20]_s$
$\lambda$	$\lambda = 30$	0.0236	0.0054	0.0184	0.0056
	$\lambda = 60$	0.0136	0.0028	0.0093	0.0028
$\eta$	$\eta = 50$	0.0136	0.0028	0.0093	0.0028
	$\eta = 150$	0.0093	0.0036	0.0072	0.0031
$\xi_0$	$\xi_0 = 10$	0.0136	0.0028	0.0093	0.0028
	$\xi_0 = 20$	0.0154	0.0028	0.0093	0.0028
$\xi_1$	$\xi_1 = 0.09$	0.0136	0.0028	0.0093	0.0028
	$\xi_1 = 0.18$	0.0166	0.0030	0.0126	0.0054